MOLECULAR AND CELLULAR BIOLOGY, May 2011, p. 2162–2170 Vol. 31, No. 10
0270-7306/11/$12.00 doi:10.1128/MCB.05234-11

Podocyte-Specific Deletion of *Myh9* Encoding Nonmuscle Myosin Heavy Chain 2A Predisposes Mice to Glomerulopathy▽

Duncan B. Johnstone,[1] Jidong Zhang,[1] Britta George,[1] Catherine Léon,[2] Christian Gachet,[2] Hetty Wong,[1] Rulan Parekh,[3] and Lawrence B. Holzman[1]*

Renal, Electrolyte and Hypertension Division, University of Pennsylvania School of Medicine, 380 South University Ave., Philadelphia, Pennsylvania 19104-4539[1]; UMR_S949 INSERM-Université de Strasbourg, Etablissement Français du Sang-Alsace, Strasbourg, France[2]; and Hospital for Sick Children, Toronto, Ontario, Canada[3]

Received 17 February 2011/Accepted 25 February 2011

Genome-wide association studies linked single-nucleotide polymorphisms (SNPs) at the *MYH9* locus to chronic kidney disease among African-Americans, particularly glomerular diseases such as HIV nephropathy and idiopathic focal and segmental glomerulosclerosis (FSGS). However, these *MYH9* SNPs are intronic, and despite extensive sequencing, a causal variant remains elusive. To investigate the role of *MYH9* in kidney disease, we selectively deleted *Myh9* from mouse podocytes and found that mutant C57BL/6 mice did not develop renal insufficiency or proteinuria compared to control littermates, even when the mice were aged for 9 months. To explain the surprisingly normal phenotype, we considered genetic redundancy with the paralog *Myh10* in podocytes, but we found that *Myh10* was not expressed in podocytes in *Myh9*-deficient or control mice. We tested whether *Myh9* podocyte deletion predisposed mice to glomerulopathy in response to injury by doxorubicin hydrochloride (Adriamycin), and we found that *Myh9* podocyte-deleted mice developed proteinuria and glomerulosclerosis, while control mice were resistant. In summary, *Myh9* podocyte deletion in C57BL/6 mice results in susceptibility to experimental doxorubicin hydrochloride glomerulopathy. We review evidence that *MYH9* dysfunction in humans results in similar susceptibility and place our data, the first examination of *Myh9* kidney disease in experimental animals, in the context of recent findings in human kidney disease, including the role of *APOL1*.

MYH9 was identified in 2008 in two genome-wide association studies (GWAS) as the major genetic locus for susceptibility to end-stage renal disease (ESRD) in African-Americans (14, 15). These studies demonstrated that multiple noncoding single-nucleotide polymorphisms (SNPs) comprising an E1 "risk haplotype" are linked to nondiabetic ESRD, hypertensive nephrosclerosis, and, in particular, glomerular diseases such as HIV nephropathy (HIVAN) and idiopathic focal and segmental glomerulosclerosis (FSGS). The data in these studies are sufficiently robust that by combining allele frequencies and odds ratios for ESRD due to *MYH9* risk alleles, this single locus can account for the fact that African-Americans develop ESRD at 3 to 4 times the rate of European-Americans (14, 15). Interest in the potential significance of *MYH9* and chronic kidney disease (CKD) has resulted in several review articles (9, 22, 30) and an NIH symposium on *Myh9* (conducted in April 2010). At the same time, two groups recently reported that CKD among African-Americans might not be linked to *MYH9* but to *APOL1*, the gene located immediately 3′ on chromosome 22 (11, 31). Aspects of these *APOL1* analyses are compelling. However, there remains no evidence that *APOL1* mutations cause CKD, and data from the human protein atlas suggest that APOL1 is not expressed in glomeruli.

MYH9 is an attractive candidate gene for susceptibility to glomerular disease and ESRD, and further study of *MYH9* is warranted. First, additional genome-wide analyses have supported the initial findings, demonstrating *MYH9* linkage to African-Americans with hypertension and albuminuria (8) and to nondiabetic ESRD in Hispanic Americans (3). Second, rare autosomal dominant *MYH9* missense mutations result in one of four giant platelet syndromes, which are now united under the rubric "Myh9-related disease" (28). All of these patients develop macrothrombocytopenia, and about 1/3 develop severe glomerular disease, termed Epstein's or Fetchner's syndrome, which progresses to ESRD requiring dialysis by young adulthood. Hence, the supposition arises that if "strong" *MYH9* missense mutations can cause severe glomerular disease, then perhaps the *MYH9* risk haplotypes are "weak" alleles that increase the likelihood of CKD later in life. This supposition is analogous to the genetic analysis of common, moderate hypercholesterolemia by looking for weak, hypomorphic alleles of genes that, when completely disrupted, result in severe hypercholesterolemia (18).

However, enthusiasm for a causal relationship between *MYH9* and kidney disease remains tempered by the fact that the *MYH9* polymorphisms linked to ESRD, including the E1, F1, and S1 haplotypes, are noncoding SNPs. Despite extensive sequencing by several groups, definitive causal sequence variants remain elusive (21), and until the search identifies a nonsynonymous polymorphism or demonstrates that intronic SNPs result in changes in transcription or splicing or in any way alter the amount or activity of MYH9 protein, the significance of the linkage between *MYH9* alleles and common causes of ESRD remains unclear.

In addition, even in the case of rare *MYH9* missense muta-

* Corresponding author. Mailing address: Renal, Electrolyte and Hypertension Division, University of Pennsylvania School of Medicine, 380 South University Ave., Philadelphia, PA 19104-4539. Phone: (215) 573-1831. Fax: (215) 898-1830. E-mail: lholzman@upenn.edu.
▽ Published ahead of print on 14 March 2011.

tions that cause severe glomerular disease, it remains unclear how (in which cells or by what mechanisms) MYH9 dysfunction results in CKD. Classical deletion of *Myh9* in mice results in embryonic lethality at approximately embryonic day 6.5 (E6.5) due to loss of cell-cell adhesion and loss of cell movement during gastrulation, particularly in the endothelium (5). In order to study kidney disease in a viable mouse model, we considered which organ- or cell-specific *Myh9* deletion might result in kidney disease. In humans and mice, *MYH9* is expressed in most organs, and one could argue that kidney disease due to MYH9 dysfunction arises in platelets (CKD due to coagulopathy), macrophages and T cells (immune-mediated CKD or aberrant inflammatory signaling), the entire kidney, or subsets of cells within the kidney.

In our initial analysis, we chose to test two models: one based on a logical guess for where *Myh9* might act and the other using a global, inducible deletion of *Myh9*. We hypothesized that rare *MYH9* mutations and common *MYH9* "risk alleles" result in glomerular disease, including FSGS and HIVAN, by disrupting cytoskeletal dynamics in podocytes. We based this hypothesis on the supposition that podocytes should be sensitive to perturbations in MYH9 function. First, while every epithelial cell likely requires nonmuscle myosin, mammals have three paralogs (MYH9, MYH10, and MYH14); cells may express one, two, or all three, and previous studies demonstrated that podocytes express MYH9 (1). Second, podocytes are particularly sensitive to perturbations of cytoskeletal dynamics (7). In fact, most heritable glomerular diseases involve genes that regulate the actin cytoskeleton (17). MYH9 interacts dynamically with f-actin to contract the cytoskeleton, and MYH9 interacts statically with f-actin to maintain membrane tension and cell shape (27); consequently, it is plausible that MYH9 dysfunction might disrupt the cytoskeleton in podocytes. Third, the role of MYH9 in general cell biology (4) includes several processes of particular interest to podocyte biology: MYH9 disruption interferes with cell-cell adhesion, which is relevant because the podocyte intercellular junction is molecularly similar to adherens junctions (25) and tight junctions (10); MYH9 disruption interferes with cell migration, which is a newly appreciated activity of podocytes visualized *in vivo* (24); and nonmuscle myosins are involved in determining cell polarity (both apical-basolateral and planar), which recent data suggest is critical during podocyte development and possibly during the response to injury (29). Finally, in humans, rare *MYH9* missense mutations result in glomerulosclerosis (26), and the strongest predisposition with common *MYH9* risk alleles is for FSGS or HIVAN; all of these are principally diseases of the podocyte.

In this report, we describe the selective deletion of *Myh9* from podocytes in C57BL/6 mice in order to better understand the relationship between MYH9 and kidney disease.

MATERIALS AND METHODS

Animal breeding and sample collection. *Myh9flox* mice were generated as described previously (16), *Pod*::*Cre* mice were generated as described previously (19), and UBC-cre/ERt2 mice were purchased from Jax. All mice were backcrossed to the C57BL/6 background. Breeding was in keeping with IACUC guidelines at the University of Michigan or University of Pennsylvania. Genomic DNAs from tails were prepared in PCR buffer (Viagen) plus 1 mg/ml proteinase K and amplified with 2× Go-*Taq* (Promega), using primers for *Myh9* (16) and *Pod*::*Cre* (19) as previously described, followed by 1.5% agarose gel electrophoresis. Each month (aged mice) or each week (doxorubicin hydrochloride [Adriamycin]-injected mice), urines were obtained from individual mice after 3 to 4 h in custom containers to keep urine free of feces; contaminated urine was discarded. Urine was spun at 4,000 × *g* for 5 min and then frozen at −20°C. Each month, urines from 12 to 14 animals of each genotype were examined by SDS-PAGE on 10% gels with Bio-Safe Coomassie blue (Bio-Rad). Urine albumin/creatinine ratios were obtained by an enzyme-linked immunosorbent assay (ELISA) plate reader (Beckman-Coulter DTX 880 reader), using a mouse Albuwell kit (Exocell) and creatinine companion (Exocell), and results were analyzed by an unpaired one-tailed *t* test (Instat). Blood from anesthetized mice, collected by retro-orbital bleed in heparinized capillary tubes (Fischer) in Microtainer serum separator tubes (BD), was analyzed by the clinical Veterinary School Pathology Laboratory of the University of Pennsylvania. Mouse blood pressure was obtained by use of a tail cuff (Visitec 2000); mice were acclimated to the device by daily training for 1 week prior to the experiment, followed by measurements for 5 days. Induction of doxorubicin hydrochloride nephropathy was done by a variant of the model of Wang, as described previously (13), by retro-orbital injection of doxorubicin hydrochloride (15 μg/g of body weight in saline) into anesthetized mice.

Mouse kidneys were prepared by perfusion with Hanks buffered salt solution (HBSS) for 3 min and then with 4% paraformaldehyde in HBSS for 15 min at 80 to 100 mm Hg retrograde into the infrarenal aorta of anesthetized mice via a 24-gauge angiocatheter (BD). After excision, kidneys were decapsulated, transected, fixed for 4 to 12 h in 4% paraformaldehyde, rinsed, and paraffin embedded by the MIA Core (University of Michigan) or Abrahamson Histology Core (University of Pennsylvania). Four-micrometer sections were made from blocks and deparaffinized with xylene-ethanol (EtOH). Antigen retrieval was optimal in 10 mM Tris, 1 mM EDTA (pH 9.0) at 65°C for >18 h. Sections were encircled by use of a Pap pen, blocked in Tris-buffered saline–0.025% Triton X-100 (TBST) plus 3% bovine serum albumin (BSA), incubated with primary antibody (Ab), washed 6 times, reblocked with TBST plus 10% goat serum (Invitrogen) plus 1% BSA, incubated with secondary Ab (Alexa Fluor–goat anti-rabbit and –goat anti-mouse [Invitrogen] at 1:1,500), washed 6 times, and mounted with Prolong Gold antifade reagent (Invitrogen). Images were obtained on Olympus IX70 microscopes using either Metamorph software (immunofluorescence [IF]) or IPLab (hematoxylin and eosin [H&E] and periodic acid-Schiff [PAS] staining) for image processing. For all IF images, we used manual rather than auto contrast, with all settings and exposures kept constant between experimental and control mice. Blinded scoring of glomerulosclerosis severity in PAS sections used a subjective scale, as follows: 1 = none/trace, 2 = mild/segmental, 3 = moderate/global, and 4 = severe sclerosis. For electron microscopy (EM), kidneys were perfusion fixed and then processed by the Biomedical Imaging Core of the University of Pennsylvania.

Primary antibodies. Anti-MYH9 (Sigma), anti-actin (Sigma), and anti-ZO1 (Zymed) were purchased from the indicated companies. Anti-MYH9 (this publication) and anti-MYH10 (this publication) were raised by injecting purified, keyhole limpet hemocyanin (KLH)-conjugated C-terminal peptides of MYH9 (SDEEVDGKADGADAKAAE) and MYH10 (DDDTESKTSDVNDTQPP QSE) into rabbits (Lampire Biologicals). Sera were purified by dialysis 3 times against 5 mM sodium phosphate buffer, pH 6.5, and then by use of Melon gel columns (Pierce). Fluorescein isothiocyanate (FITC)-tagged lectins were from Vector Labs.

Cell lines. Mouse podocytes (20), mouse mesangial cells (a gift of F. Brosius), and COS7, RBL-1, and NIH 3T3 cells were cultured at 37°C in Dulbecco's modified Eagle's medium (DMEM) plus 10% fetal bovine serum (FBS) (33°C and RPMI Glutamax for podocytes). Lysates were prepared in RIPA buffer with Complete protease inhibitor (Roche), followed by gel electrophoresis and immunoblotting as previously described (6), using horseradish peroxidase (HRP)-coupled secondary antibodies and ECL reagent (Pierce).

RESULTS

Podocyte-specific deletion of *Myh9* in C57BL/6 mice. We hypothesized that targeted deletion of *Myh9* in mouse podocytes would result in proteinuria and chronic kidney disease. Before testing this hypothesis, commercial antibodies were used to confirm that mouse podocytes express MYH9. We identified MYH9 in cultured mouse podocyte and mouse mesangial cell lines and in mouse glomerular lysate (Fig. 1A). Our negative control took advantage of the fact that COS7 cells do

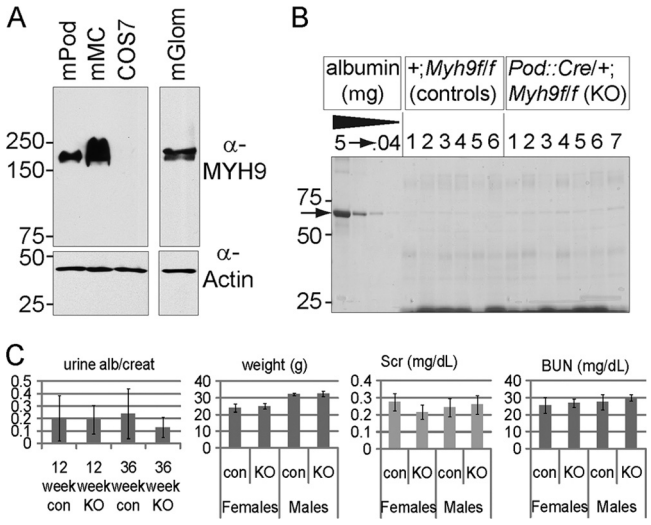

FIG. 1. Initial characterization of MYH9 in the murine kidney. (A) MYH9 immunoblot of lysates separated by SDS-PAGE. The lanes are for mouse podocytes (mPod), mouse mesangial cells (mMC), COS7 cells (which do not express MYH9), and mouse glomerular lysate (mGlom). (B) Screen for proteinuria in adult mouse urine. Shown is one of two gels with urines from 4-month-old mice of the indicated genotype, separated by SDS-PAGE and stained with Coomassie blue. Each lane is for the urine from one mouse, with a BSA standard shown on the left, in 5-fold dilutions. The arrow indicates albumin. For all urine samples, low-molecular-mass proteins of 20 to 25 kDa are visible, but albumin is barely visible (0.04 μg or less). (C) Phenotype of podocyte-specific KO mice. The left graph shows urine albumin/creatinine ratios for 12- and 36-week-old mice. In the next three graphs, for weights and serum creatinine (Scr) and blood urea nitrogen (BUN) levels of 9-month-old mice, there is no significant difference between KO and control mice (all P values are >0.1 by t test).

not express MYH9 (2). C57BL/6 mice expressing a *Pod*::*Cre* transgene (19) were crossed with BL/6 mice carrying a floxed allele of *Myh9* (16) in which loxP sites flank ATG-containing exon 2. Double heterozygous F1 offspring (*Pod*::*Cre*/+; *Myh9f*/+) were crossed to *Myh9f/f* mice. In the F2 generation, four genotypes were anticipated, each at 1/4 frequency, and from 175 weaned offspring, we observed 47 *Pod*::*Cre*/+; *Myh9f/f* (podocyte-specific knockout [KO] mice), 43 *Pod*::*Cre*/+; *Myh9f*/+ (podocyte-specific heterozygotes), 45 +/+; *Myh9f/f* (Cre^- control littermates [Con]), and 40 +/+; *Myh9f*/+ (Cre^- floxed heterozygotes) mice. This Mendelian distribution indicates that the loss of *Myh9* in podocytes does not influence survival. To test for a delayed phenotype of kidney disease, urines from 24 to 26 mice were collected each month. We found no excessive proteinuria in months 1 through 9 (Fig. 1B). To examine proteinuria quantitatively, albumin and creatinine ELISAs of mouse urine at 3 and 9 months were performed, and there was no significant difference in the urine albumin/creatinine ratios of KO versus control littermates (Fig. 1C), with a P value of >0.2 by t test. In addition, after aging mice for 9 months, there was no significant difference between KO and control mice in weight, which can decrease with uremia (Fig. 1C) ($P > 0.5$), or in serum creatinine ($P > 0.1$) or blood urea nitrogen ($P > 0.2$) levels. Lastly, after aging mice for 11 to 12 months, there was no significant difference in tail cuff blood pressure between *Myh9f/f* control mice (systolic pressure, 109.82 ± 11.3; diastolic pressure, 88.30 ± 11.2) ($n = 32$ trials with 6 mice) and KO mice (systolic pressure, 109.99 ± 13.3; diastolic pressure, 89.38 ± 16.8) ($n = 17$ trials with 4 mice).

We explored several explanations for the lack of proteinuria and chronic kidney disease in mice with podocyte-specific deletion of *Myh9*, including (but not limited to) failure to efficiently delete the *Myh9* floxed allele from podocytes, genetic redundancy in podocytes with a paralog of *Myh9*, and the possibility that a second provocative agent is required to unmask a phenotype. To establish whether efficient deletion of *Myh9* in podocytes had been achieved, primers that flanked the loxP sites were used to amplify a 318-bp deletion product from genomic DNA of the kidneys of KO mice but not from any other organ and not from control mice. However, this assay is sensitive and might generate a product if only a small fraction of podocytes carry the *Myh9* deletion. Accordingly, we looked for a loss of MYH9 protein in podocytes of KO mice by IF microscopy. Initial attempts at indirect IF using a commercially available MYH9 antibody did not confirm the deletion, but we observed that the epitope used to make this commercial antibody was derived from a region of MYH9 (amino acids 1165 to 1302) with very high amino acid identity with paralogs of MYH9 (90 of the 138 residues are identical to those in MYH10, MYH14, or both). While this antibody appeared to be specific in immunoblots for denatured MYH9 (Fig. 1), we hypothesized that this antibody might cross-react with paralogous heavy chains in the native conformation and be less specific in IF assays of MYH9. Accordingly, we raised new polyclonal antibodies against the C termini of MYH9 and MYH10; these epitopes are divergent among myosins and bear little similarity to other proteins. The resulting antibodies against MYH9 and MYH10 were purified by use of Melon gel columns (see Materials and Methods) and examined for specificity by immunoblotting (Fig. 2A), taking advantage of the fact that COS7 cells do not express MYH9, rat basophil leukemia cells do not express MYH10, and NIH 3T3 cells express both (2, 12).

The MYH9 antibodies were used to stain paraffin-embedded mouse kidneys. At low power, indirect IF revealed MYH9 in glomeruli, a subset of tubules, and interstitial cells (Fig. 2B). Staining specificity was tested without primary antibody and by preincubation of purified MYH9 C-terminal peptide with combined anti-MYH9 and anti-ZO1 antibodies, which fully competed MYH9 staining but did not alter ZO1 staining (Fig. 2B, top right panels). High-power IF revealed MYH9 in the cytoplasm of several glomerular cells, including mesangial cells and podocytes (Fig. 2B, large arrows). In kidneys from KO mice, MYH9 staining of tubules and mesangial cells remained robust, but MYH9 staining in podocytes was absent or punctate (Fig. 2B, bottom row, small arrows). We concluded that the *MYH9* floxed allele was efficiently deleted in podocytes and that there must be another explanation for the lack of proteinuria and overt CKD in KO mice.

To test whether *Myh9* is genetically redundant with *Myh10* in the podocyte, we performed indirect IF with purified MYH10 antibodies (Fig. 2A). At low power, indirect IF revealed MYH10 staining in glomeruli and rare tubules (Fig. 3, top row), a more restricted pattern than we observed with MYH9. Preincubation of purified MYH10 C-terminal peptide with a combination of anti-MYH10 and anti-ZO1 fully competed

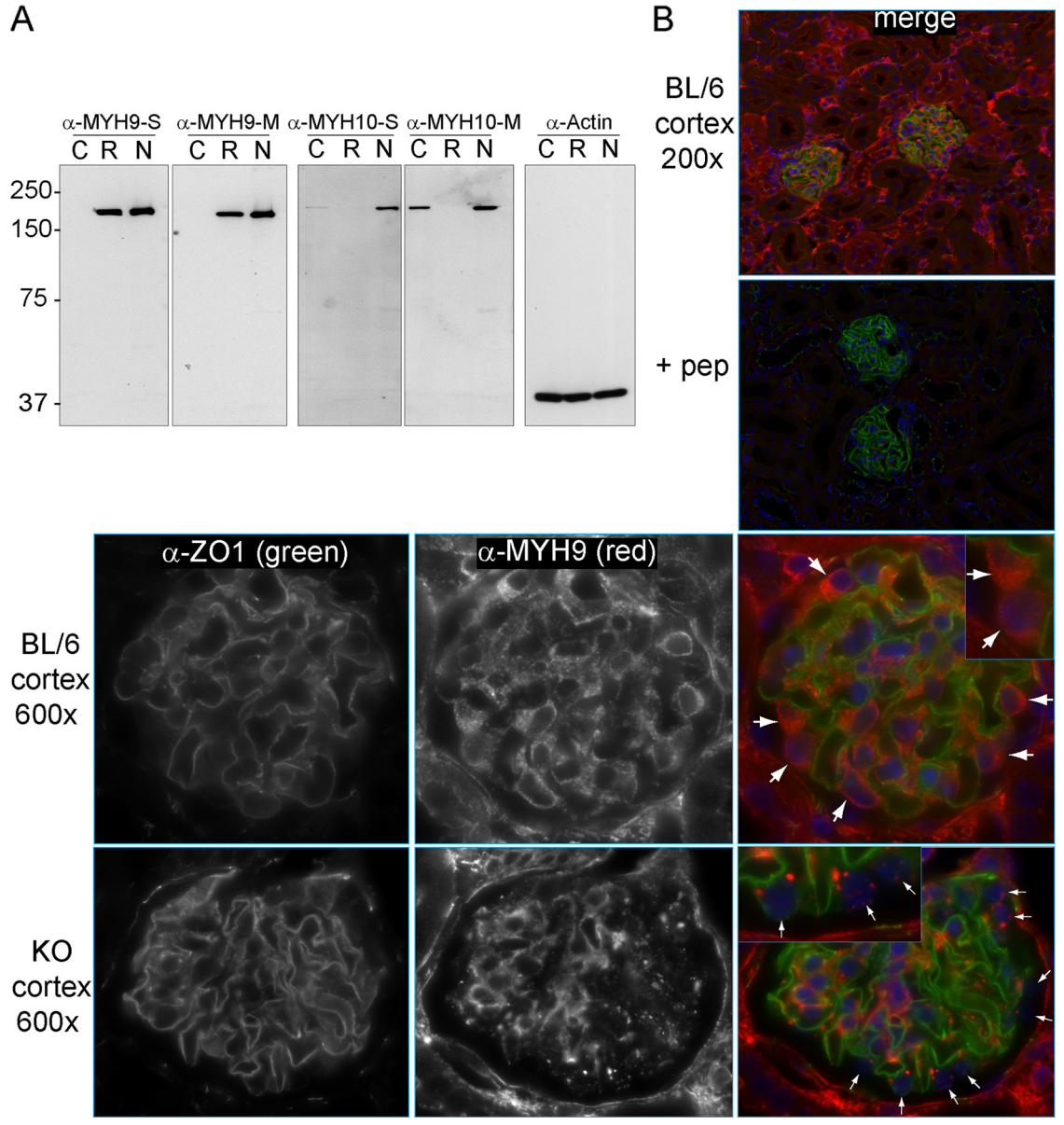

FIG. 2. Localization of MYH9 in mouse kidneys. (A) Immunoblots to characterize new anti-MYH9 and anti-MYH10 antibodies, comparing equivalent titers of crude serum (S) or Melon gel-purified antibody (M). Lysates: C, COS7 cells (which do not express MYH9); R, rat basophil leukemia cells (which do not express MYH10); and N, NIH 3T3 cells (which express both MYH9 and MYH10). (B) Indirect IF with purified anti-MYH9 (1:400) and anti-ZO1 (1:200) in perfusion-fixed kidneys. (Top right) The panel (merge) is a ×200 view demonstrating ZO1 in glomeruli and MYH9 in a subset of tubules as well as glomeruli. (Top right, second panel) MYH9 peptide (1 ng/μl) was added to the anti-MYH9 and anti-ZO1 primary Ab mix (+ pep), and with identical photo settings, there was no MYH9 staining, while ZO1 staining was unchanged. Secondary Ab-only controls were similarly dark. (Top row) A ×600 view of a glomerulus demonstrates anti-MYH9 staining of podocyte cytoplasm (large white arrows) as well as mesangial and possibly endothelial cells within the glomerulus. (Bottom row) In glomeruli from KO mice, MYH9 is no longer visible in podocytes (small white arrows), while MYH9 staining of the mesangium and other cells is unchanged.

MYH10 staining but left ZO1 staining unchanged (Fig. 3, second row). High-power images of the glomerulus showed MYH10 in mesangial cells but not in podocytes (Fig. 3, third row, small arrows). Therefore, *Myh10* is unlikely to be genetically redundant with *Myh9* in the podocyte. There are instances in which paralogous genes reciprocally suppress each other's expression, such that one might see MYH10 expression in podocytes only after loss of MYH9 expression. However, as in wild-type BL/6 mice, MYH10 expression was not observed in podocytes of KO mice (Fig. 3, bottom row). We concluded that *Myh10* is not genetically redundant with *Myh9* in podocytes, and we sought an alternative explanation for the lack of phenotype in KO mice.

We considered whether MYH9-related CKD might arise from MYH9 dysfunction in kidney cells in addition to podocytes (e.g., tubular epithelial or mesangial cells) or in cells of other organs known to cause CKD (platelets or leukocytes) or might be due to a developmental role for MYH9. To address

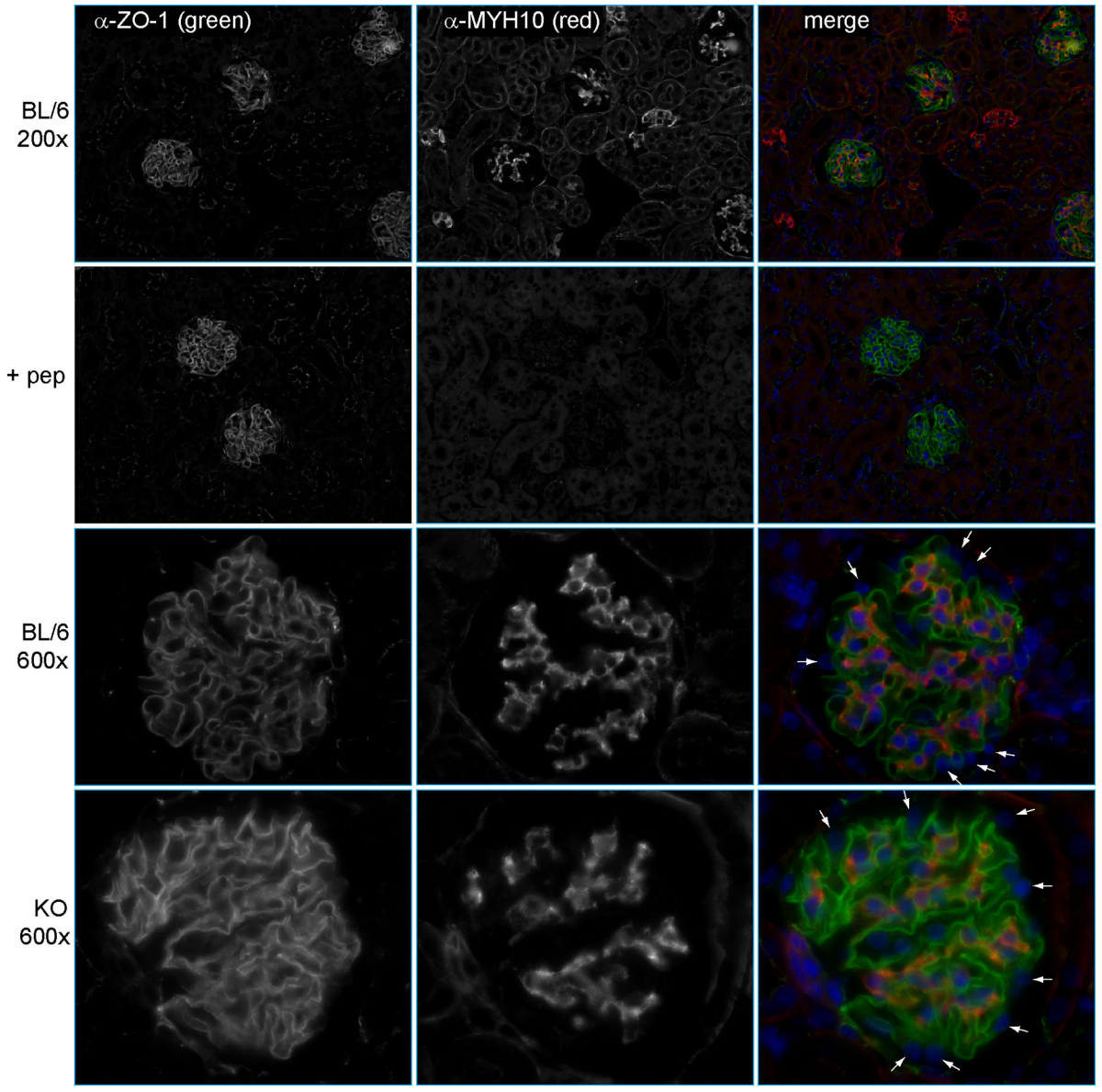

FIG. 3. Localization of MYH10 in mouse kidneys. Indirect IF was performed with anti-MYH10 (1:800), as characterized by immunoblotting in Fig. 2A, and anti-ZO1 (1:200). (Top row) Images at a magnification of ×200 show MYH10 in glomeruli and rare tubules. (Second row) MYH10 peptide (0.2 ng/μl) was added to the anti-MYH10 and anti-ZO1 primary Ab mix (+ pep). With identical photo settings, MYH10 staining was competed away while ZO1 staining was unchanged. (Third row) Images of glomeruli at a magnification of ×600 reveal MYH10 in mesangial cells but not in podocytes (small white arrows). (Bottom row) MYH10 expression in kidneys of KO mice is unchanged from that in controls, with prominent mesangial staining and no staining of podocytes (small white arrows).

the many possibilities, mice bearing the ubiquitously expressed *UBC*::*Cre*/*ERT2* transgene were bred with *Myh9f*/*f* mice to obtain mice in which *Myh9* was conditionally deleted in all tissues upon exposure to tamoxifen, administered before or after kidney development. In initial experiments, two groups of mice (*UBC*::*Cre*/*ERT2*/+; *Myh9f*/*f* mice and control littermates) were aged to 3 months and then exposed to tamoxifen. All experimental mice ($n = 8$) died within 3 days of tamoxifen exposure, whereas control mice ($n = 7$) remained unaffected for over 21 days after tamoxifen exposure. Similarly, mice of both genotypes exposed to vehicle alone ($n = 5$) were unaffected. While these results point to the necessity of MYH9 postdevelopment, this experimental model did not allow examination of kidney disease in mice.

Podocyte KO mice are predisposed to doxorubicin hydrochloride-induced FSGS. We hypothesized that the loss of *Myh9* in podocytes alone is not sufficient to cause a podocytopathy or overt glomerular disease but predisposes individuals to disease in response to a second environmental or genetic stress. To test this hypothesis, we chose to examine the susceptibility of mutant and wild-type BL/6 mice to doxorubicin hydrochloride as a general means of stressing podocytes. Moderate doses of doxorubicin hydrochloride (10.5 μg/g) result in significant glomerular disease in susceptible strains such as

BALB/c, whereas the C57BL/6 strain is resistant (29). Mice of 9 to 11 months of age on the BL/6 background with no significant proteinuria at the onset of the experiment (Fig. 4B, wk 0) were injected with either 15 μg/g of doxorubicin hydrochloride (in saline) or equal volumes of saline. Six experimental groups were examined: KO mice (*Pod*::*Cre*/+; *Myh9f/f* mice injected with doxorubicin hydrochloride or saline [groups 1 and 2]), ff control mice (Cre^-; *Myh9f/f* mice injected with doxorubicin hydrochloride or saline [groups 3 and 4]), and PCre control mice ($PCre^+$; $Myh9^{+/+}$ mice injected with doxorubicin hydrochloride or saline [groups 5 and 6; these mice were 4 months old at the time of injection]). Urine was screened by Coomassie blue staining and SDS-PAGE, and from week 2 through week 6, we observed heavy albuminuria in doxorubicin hydrochloride-injected KO mice (Fig. 4A). Quantification of albuminuria by ELISA revealed that KO mice injected with doxorubicin hydrochloride developed significant albuminuria at weeks 3, 4, and 6 compared to KO mice injected with saline (Fig. 4B). More importantly, KO mice injected with doxorubicin hydrochloride developed more albuminuria than control mice receiving doxorubicin hydrochloride injection at weeks 3, 4, and 6 (Fig. 4B). Although there was phenotypic variability resulting in a large standard deviation, possibly from vascular effects seen with intravenous doxorubicin hydrochloride injection, we found severe nephropathy only in KO mice injected with doxorubicin hydrochloride.

After 6 weeks, two mice from each experimental group were sacrificed for histological examination of perfusion-fixed kidneys. Doxorubicin hydrochloride injection of KO mice revealed focal and segmental glomerulosclerosis by both H&E and PAS staining, with glomerular changes ranging from mild segmental sclerosis to severe global sclerosis (Fig. 4C, top row), numerous proteinaceous casts, and an interstitial hypercellularity. In control mice injected with doxorubicin hydrochloride, there were foci of mild sclerosis but no globally sclerotic glomeruli (Fig. 4C, second and third rows), while saline injection into KO or control mice did not cause significant glomerulosclerosis. Semiquantitative, blinded scoring of glomerulosclerosis severity in sections from each experimental group revealed a median severity score of 3 for glomeruli from KO mice injected with doxorubicin hydrochloride ($n = 246$ glomeruli), which was significantly different from those for the other five groups, each of which had a median severity score of 1 (Fig. 4D).

Scanning EM (SEM) of glomeruli of KO mice injected with doxorubicin hydrochloride revealed patches of foot process widening and foot process fusion (Fig. 5, 1st row, left panel) and areas consistent with pseudovillous transformation. For comparison, foot process fusion was not observed by SEM for control mice injected with doxorubicin hydrochloride (Fig. 5, 2nd and 3rd rows, left panels). Foot processes of KO mice, ff control mice, and $PCre^+$ mice injected with saline were well spaced and structurally preserved (Fig. 5, 4th row, left panel). Similarly, transmission electron microscopy of KO mice injected with doxorubicin hydrochloride revealed patches of severe foot process effacement and, in some glomerular loops, thickening of the basement membrane (Fig. 5, 1st row, right panel). In control mice injected with doxorubicin hydrochloride and in mice of all genotypes injected with saline, there was no evidence of severe foot process effacement or basement membrane thickening (Fig. 5, rows 2 to 4, right panels). In summary, in mice with podocyte-specific deletion of *Myh9*, provocation with doxorubicin hydrochloride resulted in severe albuminuria, FSGS by light microscopy, foot process fusion, and foot process effacement by electron microscopy. We concluded that podocyte-specific deletion of *Myh9* predisposes mice to glomerular disease in response to a mouse model of podocyte injury.

DISCUSSION

Our study of the relationship between *Myh9* and kidney disease in mice was motivated by the recent identification of *MYH9* as a susceptibility locus for common forms of CKD in African-Americans, including hypertensive nephrosclerosis, nondiabetic ESRD, and particularly the glomerular diseases FSGS and HIV-associated nephropathy. *MYH9* is an attractive candidate for a susceptibility gene for common forms of CKD, as rare missense mutations in *MYH9* are known to cause glomerular disease in patients with Epstein's and Fetchner's syndrome. In the debate over the nature of inheritance in human disease, this would be an instance in which rare variants at a single genetic locus cause rare disease and common mild variants cause common disease. In this study, we hypothesized that MYH9 dysfunction in podocytes causes kidney disease in cases of both rare *MYH9* missense mutations and common *MYH9* "risk haplotypes." To our surprise, we found that podocyte-specific deletion of *Myh9* was not sufficient to cause proteinuria or CKD in BL/6 mice but predisposed mice to disease after a second provocation. In this instance, doxorubicin hydrochloride resulted in significant proteinuria and FSGS in KO mice.

Similar to our results for mice, a review of the literature on *MYH9*-related disease in humans suggests that the development of kidney disease requires a second provocation. First, in the reports linking common *MYH9* alleles to common CKD in African-Americans, the E1 haplotype frequency was 84 to 93% in persons with FSGS and HIVAN but 60 to 70% in persons without CKD (15), high enough to suggest that while the *MYH9* risk haplotype may predispose many African-Americans to CKD, it is not sufficient to cause CKD. Similarly, missense mutations in *MYH9* in autosomal dominant Epstein's and Fetchner's syndromes also appear to be predisposing agents but not sufficient to cause CKD. Most clearly supporting this contention is the published description of a family with Fetchner's syndrome in which 10 family members had the same missense mutation in *MYH9* (D1424H) and all had the platelet phenotype of macrothrombocytopenia (28). Among adults in this family, two had Fetchner's syndrome with nephrosis-range proteinuria and ESRD requiring dialysis as young adults, while five relatives of similar or greater age had the same degree of macrothrombocytopenia but no proteinuria or abnormal serum creatinine. Incredibly, members of this family with the D1424H mutation either developed severe glomerular disease requiring dialysis or did not have kidney disease; no family member had an intermediate phenotype of moderate proteinuria or moderate CKD. In the case of this family with rare Fetchner's syndrome, and in the case of the common *MYH9* risk haplotype among African-Americans, it appears that *MYH9* mutations might predispose individuals to CKD but are not sufficient to create it, and we suggest that a second prov-

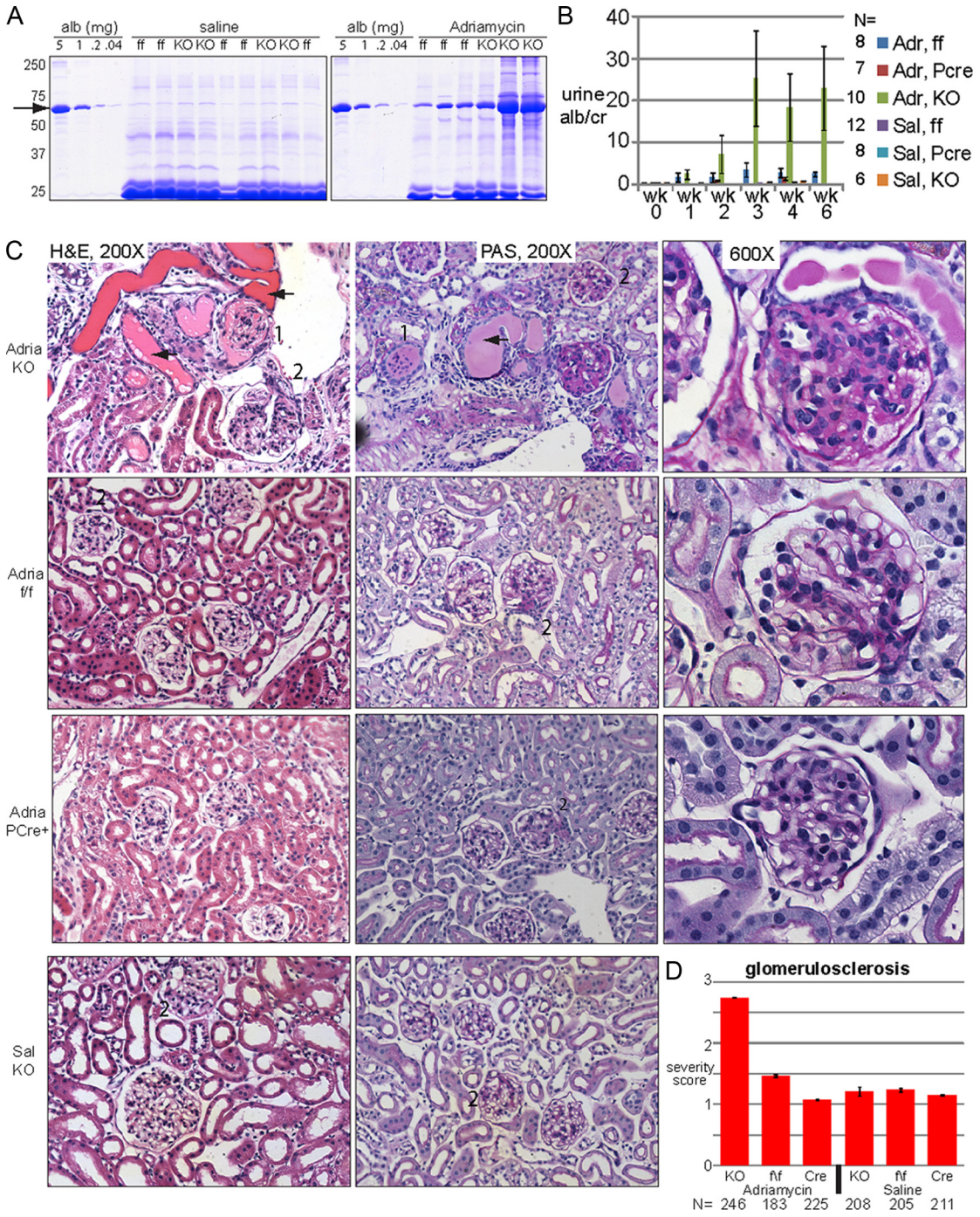

FIG. 4. Podocyte-specific KO mice are predisposed to doxorubicin hydrochloride-induced nephropathy. KO, knockout mice (*Pod*::*Cre*/+; *Myh9f/f*); ff, control mice (+; *Myh9f/f*); PCre, control mice (*PCre*; +/+); Adr, doxorubicin hydrochloride (Adriamycin) in saline; Sal, saline only. (A) Coomassie blue-stained SDS-PAGE gel with urines 2 weeks after injection of saline or doxorubicin hydrochloride. An albumin standard is shown at 5-fold dilutions, with the arrow indicating albumin. All urines with heavy albuminuria were from KO animals. (B) Urine ELISA albumin/creatinine ratios after injection of mice with saline or doxorubicin hydrochloride (means ± standard errors of the means). Doxorubicin hydrochloride-treated KO mice had more albuminuria than all other groups at weeks 3, 4, and 6 (Welsch's *t* test [unpaired, not assuming equal variances, and one-tailed]). All pairwise combinations with doxorubicin hydrochloride-treated KO mice had *P* values of 0.05 or less, although due to the large standard error of the mean, the significance was borderline for doxorubicin hydrochloride-treated KO versus doxorubicin hydrochloride-treated ff mice at 4 weeks (*P* value = 0.0524) and for doxorubicin hydrochloride-treated KO versus doxorubicin hydrochloride-treated ff mice at 3 weeks (*P* value = 0.0526). (C) KO mice develop focal and segmental glomerulosclerosis. Some images were removed to accommodate available space. 1, global sclerosis; 2, segmental sclerosis; arrow, proteinaceous cast. Images for ff control mice and $PCre^{+}$ mice injected with saline were similar to those for KO mice injected with saline and are not shown. (D) Mean glomerulosclerosis severity scores (± standard deviations), judged blindly, albeit subjectively (1 to 4+), for two mice for each condition. N, total number of glomeruli. Median scores are reported in Results. By the nonparametric Mann-Whitney test, there was no difference between saline-treated groups or between *PCre* controls treated with doxorubicin hydrochloride versus saline, but there was a significant difference between KO mice treated with doxorubicin hydrochloride and every other group ($P < 1e{-}6$).

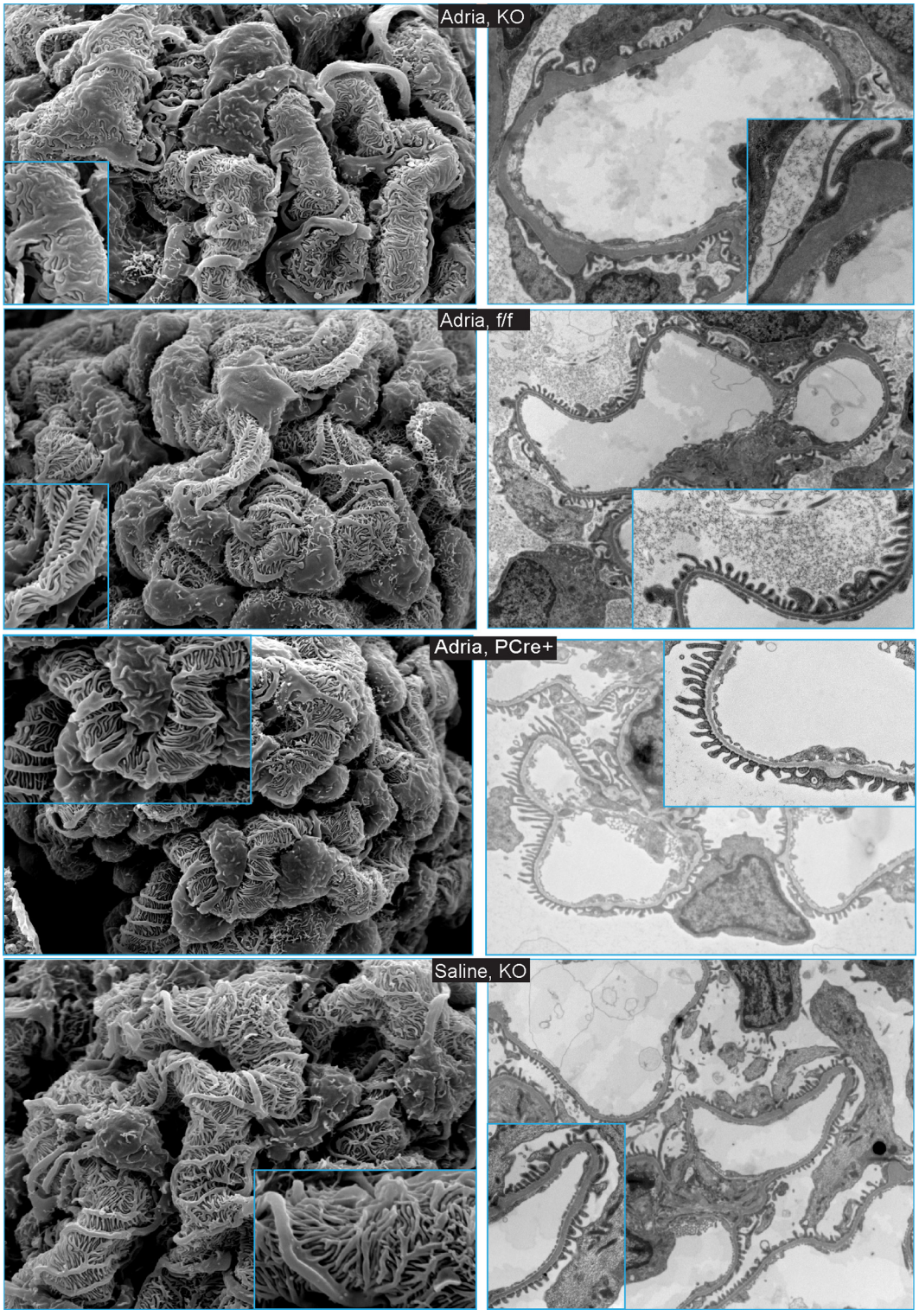

FIG. 5. Scanning electron microscopy (left panels) and transmission electron microscopy (right panels) reveal changes in foot process architecture in KO mice injected with doxorubicin hydrochloride. Scanning EM of glomeruli was performed at low power (×3,000) and high power (inset; ×10,000). Transmission EM images were obtained at low power (×6,000 to ×7,500) and high power (inset; ×15,000 to ×25,000). Genotypes are indicated in the center of each row. Images for ff control mice and $PCre^{+}$ control mice injected with saline were similar to those for KO mice injected with saline and are not shown.

ocation, either environmental (e.g., HIV exposure) or genetic (second-site noncomplementation in podocytes), is necessary to develop *MYH9*-related CKD. To uncover potential genes interacting with *MYH9* in humans with kidney disease, one could examine families with *MYH9* missense mutations or groups with *MYH9* risk haplotypes and look for further genetic differences between affected and unaffected persons. Similarly, if there are significant differences among mouse strains in susceptibility to *MYH9*-related kidney disease, this could be exploited to uncover candidate genetic loci, as elegantly demonstrated in a study of differential susceptibility to HIV nephropathy among mouse strains (23).

Lastly, in the course of writing this report, dramatic new results from two research groups suggested that kidney disease among African-Americans is linked not to *MYH9* but to *APOL1*, which lies at the 3′ end of *MYH9* and is in high linkage disequilibrium (11, 31). Given the difficulty in identifying causal variants in the *MYH9* risk haplotypes, the *APOL1* data are compelling because the relevant SNPs are missense mutations and are predicted to confer resistance to human African trypanosomiasis caused by *Trypanosoma brucei rhodesiense*. In the model proposed by these two groups, heterozygous mutations at *APOL1* confer resistance to trypanosomiasis and positively select these alleles, while homozygous mutations, akin to the case for sickle cell disease, confer a deleterious phenotype of CKD. Still, there are a few weaknesses in the *APOL1* story. While the *APOL1* "missense risk haplotype" is common among African-Americans and West African Yorubans, the selective advantage conferred by this haplotype is resistance toward a trypanosome endemic to East and Southern Africa. Second, there is no evidence that *APOL1* mutations can cause kidney disease, and in fact, APOL1 does not appear to be expressed in the glomerulus, according to the human protein atlas. In sum, the data supporting *MYH9* or *APOL1* as a candidate gene for kidney disease complement each other: the *APOL1* haplotype is highly correlated with ESRD and includes missense mutations, and positive selection to trypanosomiasis may explain the high allele frequency observed, while in the closely linked *MYH9* locus, missense mutations can cause glomerular disease. It is possible that African variant alleles of *APOL1* (G1 and G2) confer positive selection of alleles while kidney disease in this population arises from something other than *APOL1* variants which is in high linkage disequilibrium. Until additional studies demonstrate the cause of kidney disease in African ancestral populations, we suggest that studies of both loci are warranted.

ACKNOWLEDGMENTS

Grants from Nephcure and NIDDK (to D.B.J.), from Deutsche FG to B.G., and from NIDDK and the Department of Veterans Affairs (to L.B.H.) supported this work.

We thank J. R. Sedor and L. A. Bruggeman for advice and encouragement, T. B. Huber and B. Hartleben for the Adriamycin protocol, and members of the Animal Model Core (University of Pennsylvania) for use of the Visitec 2000 device.

REFERENCES

1. **Arrondel, C., et al.** 2002. Expression of the nonmuscle myosin heavy chain IIA in the human kidney and screening for MYH9 mutations in Epstein and Fechtner syndromes. J. Am. Soc. Nephrol. **13:**65–74.
2. **Bao, J., S. S. Jana, and R. S. Adelstein.** 2005. Vertebrate nonmuscle myosin II isoforms rescue small interfering RNA-induced defects in COS-7 cell cytokinesis. J. Biol. Chem. **280:**19594–19599.
3. **Behar, D. M., et al.** 2010. African ancestry allelic variation at the MYH9 gene contributes to increased susceptibility to non-diabetic end-stage kidney disease in Hispanic Americans. Hum. Mol. Genet. **19:**1816–1827.
4. **Conti, M. A., and R. S. Adelstein.** 2008. Nonmuscle myosin II moves in new directions. J. Cell Sci. **121:**11–18.
5. **Conti, M. A., S. Even-Ram, C. Liu, K. M. Yamada, and R. S. Adelstein.** 2004. Defects in cell adhesion and the visceral endoderm following ablation of nonmuscle myosin heavy chain II-A in mice. J. Biol. Chem. **279:**41263–41266.
6. **Fan, G., S. E. Merritt, M. Kortenjann, P. E. Shaw, and L. B. Holzman.** 1996. Dual leucine zipper-bearing kinase (DLK) activates p46SAPK and p38mapk but not ERK2. J. Biol. Chem. **271:**24788–24793.
7. **Faul, C., K. Asanuma, E. Yanagida-Asanuma, K. Kim, and P. Mundel.** 2007. Actin up: regulation of podocyte structure and function by components of the actin cytoskeleton. Trends Cell Biol. **17:**428–437.
8. **Freedman, B. I., et al.** 2009. Polymorphisms in the nonmuscle myosin heavy chain 9 gene (MYH9) are associated with albuminuria in hypertensive African Americans: the HyperGEN study. Am. J. Nephrol. **29:**626–632.
9. **Freedman, B. I., and J. R. Sedor.** 2008. Hypertension-associated kidney disease: perhaps no more. J. Am. Soc. Nephrol. **19:**2047–2051.
10. **Fukasawa, H., S. Bornheimer, K. Kudlicka, and M. G. Farquhar.** 2009. Slit diaphragms contain tight junction proteins. J. Am. Soc. Nephrol. **20:**1491–1503.
11. **Genovese, G., et al.** 2010. Association of trypanolytic ApoL1 variants with kidney disease in African-Americans. Science **329:**841–845.
12. **Golomb, E., et al.** 2004. Identification and characterization of nonmuscle myosin II-C, a new member of the myosin II family. J. Biol. Chem. **279:**2800–2808.
13. **Hartleben, B., et al.** 2010. Autophagy influences glomerular disease susceptibility and maintains podocyte homeostasis in aging mice. J. Clin. Invest. **120:**1084–1096.
14. **Kao, W. H., et al.** 2008. MYH9 is associated with nondiabetic end-stage renal disease in African Americans. Nat. Genet. **40:**1185–1192.
15. **Kopp, J. B., et al.** 2008. MYH9 is a major-effect risk gene for focal segmental glomerulosclerosis. Nat. Genet. **40:**1175–1184.
16. **Leon, C., et al.** 2007. Megakaryocyte-restricted MYH9 inactivation dramatically affects hemostasis while preserving platelet aggregation and secretion. Blood **110:**3183–3191.
17. **Machuca, E., G. Benoit, and C. Antignac.** 2009. Genetics of nephrotic syndrome: connecting molecular genetics to podocyte physiology. Hum. Mol. Genet. **18:**R185–R194.
18. **McClellan, J., and M. C. King.** 2010. Genetic heterogeneity in human disease. Cell **141:**210–217.
19. **Moeller, M. J., S. K. Sanden, A. Soofi, R. C. Wiggins, and L. B. Holzman.** 2003. Podocyte-specific expression of cre recombinase in transgenic mice. Genesis **35:**39–42.
20. **Mundel, P., et al.** 1997. Rearrangements of the cytoskeleton and cell contacts induce process formation during differentiation of conditionally immortalized mouse podocyte cell lines. Exp. Cell Res. **236:**248–258.
21. **Nelson, G. W., et al.** 2010. Dense mapping of MYH9 localizes the strongest kidney disease associations to the region of introns 13 to 15. Hum. Mol. Genet. **19:**1805–1815.
22. **Nunez, M., A. M. Saran, and B. I. Freedman.** 2010. Gene-gene and gene-environment interactions in HIV-associated nephropathy: a focus on the MYH9 nephropathy susceptibility gene. Adv. Chronic Kidney Dis. **17:**44–51.
23. **Papeta, N., et al.** 2009. Susceptibility loci for murine HIV-associated nephropathy encode trans-regulators of podocyte gene expression. J. Clin. Invest. **119:**1178–1188.
24. **Peti-Peterdi, J., and A. Sipos.** 2010. A high-powered view of the filtration barrier. J. Am. Soc. Nephrol. **21:**1835–1841.
25. **Reiser, J., W. Kriz, M. Kretzler, and P. Mundel.** 2000. The glomerular slit diaphragm is a modified adherens junction. J. Am. Soc. Nephrol. **11:**1–8.
26. **Sekine, T., et al.** 2010. Patients with Epstein-Fechtner syndromes owing to MYH9 R702 mutations develop progressive proteinuric renal disease. Kidney Int. **78:**207–214.
27. **Sellers, J. R.** 2000. Myosins: a diverse superfamily. Biochim. Biophys. Acta **1496:**3–22.
28. **Seri, M., et al.** 2003. MYH9-related disease: May-Hegglin anomaly, Sebastian syndrome, Fechtner syndrome, and Epstein syndrome are not distinct entities but represent a variable expression of a single illness. Medicine (Baltimore) **82:**203–215.
29. **Simons, M., B. Hartleben, and T. B. Huber.** 2009. Podocyte polarity signalling. Curr. Opin. Nephrol. Hypertens. **18:**324–330.
30. **Singh, N., N. Nainani, P. Arora, and R. C. Venuto.** 2009. CKD in MYH9-related disorders. Am. J. Kidney Dis. **54:**732–740.
31. **Tzur, S., et al.** 2010. Missense mutations in the APOL1 gene are highly associated with end stage kidney disease risk previously attributed to the MYH9 gene. Hum. Genet. **128:**345–350.